

Stellar Properties of the Host Galaxy of an Ultraluminous X-ray Source in NGC 5252

Minjin Kim,¹★ Kristhell M. López,^{2,3} Peter G. Jonker,^{2,3} Luis C. Ho,^{4,5} and Myungshin Im

¹*Department of Astronomy and Atmospheric Sciences, Kyungpook National University, Daegu 41566, Republic of Korea*

²*SRON Netherlands Institute for Space Research, Sorbonnelaan 2, NL-3584 CA Utrecht, the Netherlands*

³*Department of Astrophysics/IMAPP, Radboud University, PO Box 9010, NL-6500 GL Nijmegen, the Netherlands*

⁴*Kavli Institute for Astronomy and Astrophysics, Peking University, Beijing 100871, China*

⁵*Department of Astronomy, School of Physics, Peking University, Beijing 100871, China*

⁶*Astronomy Program, FPRD, Department of Physics & Astronomy, Seoul National University, 1 Gwanak-ro, Gwanak-gu, Seoul 08826, Republic of Korea*

Accepted XXX. Received YYY; in original form ZZZ

ABSTRACT

An ultraluminous X-ray source (ULX) in NGC 5252 has been known as a strong candidate for an off-nuclear intermediate-mass black hole. We present near-infrared imaging data of the ULX obtained with the William Herschel Telescope. Using this data we estimate a stellar mass associated with the ULX of $\approx 10^{7.9\pm 0.1} M_{\odot}$, suggesting that it could be (the remnant of) a dwarf galaxy that is in the process of merging with NGC 5252. Based on a correlation between the mass of the central black hole (BH) and host galaxy, the ULX is powered by a $10^5 M_{\odot}$ black hole. Alternatively, if the BH mass is $\approx 10^6 M_{\odot}$ or larger, the host galaxy of the ULX must have been heavily stripped during the merger. The ULX K_s -band luminosity is two orders of magnitude smaller than that expected from an ordinary active galactic nucleus with the observed [O III] luminosity, which also suggests the ULX lacks a dusty torus. We discuss how these findings provide suggestive evidence that the ULX is hosting an intermediate-mass black hole.

Key words: galaxies: active — galaxies: individual (NGC 5252) — galaxies: Seyfert — X-rays: galaxies — black hole physics

1 INTRODUCTION

Supermassive black holes (SMBHs) are nearly always present in the nuclei of massive galaxies, and they are thought to play an important role in the formation and evolution of the host galaxy. This is for instance inferred from the strong correlation between SMBH mass and host galaxy stellar mass (e.g. Kormendy & Ho 2013). However, it remains unclear how SMBHs are formed and evolve in the early universe. Recent observational studies of high- z quasars showed that some SMBHs are already as massive as $10^{8-9} M_{\odot}$ when the age of the universe was around 0.7–0.8 Gyr (e.g. Mortlock et al. 2011; Bañados et al. 2018). The seed BH mass is a critically important parameter which depends on its formation mechanism. It ranges from approximately 10^2 to $10^5 M_{\odot}$ (Volonteri 2010; Mezcua 2017), suggesting that intermediate-mass black holes (IMBHs) could be the building blocks of SMBHs. However, despite their importance, highly accreting IMBHs are rare in the present universe (e.g. Greene & Ho 2004), although IMBHs

with low accretion rate may be relatively common (e.g. Miller et al. 2015; She et al. 2017).

The possibility to find an IMBH is a strong motivation to study ultraluminous X-ray sources (ULX; $L_{X\text{-ray}} \geq 10^{39}$ erg s^{-1}). By definition, the X-ray luminosity of a ULX exceeds the Eddington luminosity of a $10 M_{\odot}$ stellar-mass black hole, and it does not reside in the nucleus of the apparent host galaxy. Observational studies suggest that ULXs are preferentially found in low-mass or star-forming galaxies (e.g. Swartz et al. 2004; Walton et al. 2011). Such high star-formation rate and low metallicity environments are expected to form massive stellar BHs efficiently. Therefore, a ULX may represent extreme cases of accreting stellar-mass BHs (i.e. X-ray binaries). Theoretical studies also argue that the ULX X-ray luminosity can be amplified due to beaming effects (King et al. 2001), further supporting the concept that a stellar-mass BH is the origin of many ULXs.

Furthermore, some ULXs show coherent pulsations indicating it is powered by accretion onto a neutron star (e.g. Bachetti et al. 2014; Furst et al. 2016; Israel et al. 2017; Brightman et al. 2018). Nevertheless, a few ULXs including hyperluminous X-ray sources (HLXs; $L_{X\text{-ray}} \geq$

★ E-mail: mkim.astro@gmail.com (MK)

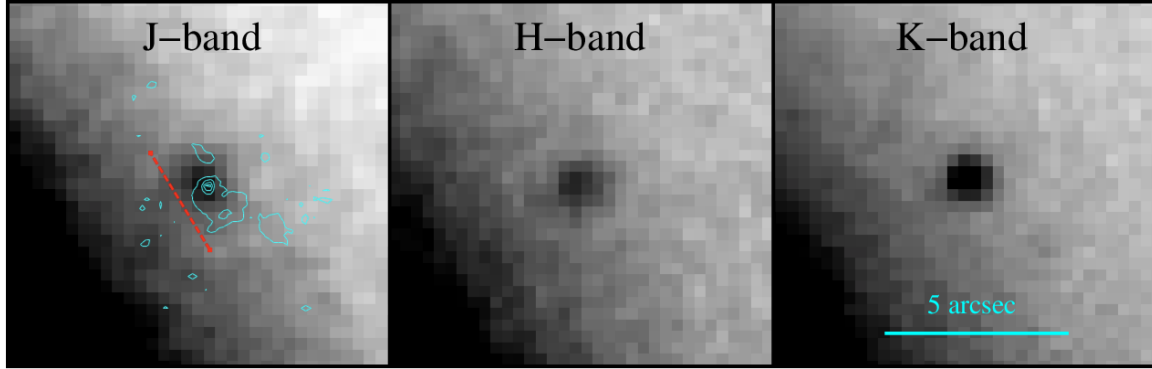


Figure 1. Postage stamp images for CXO J133815.6+043255 in J , H , and K_s from left to right (North is up and East is left). The background gradient is due to the stellar light from the host galaxy (NGC 5252). Left panel: the overlaid contour represents the $H\alpha$ flux distribution which estimated from the *HST* image obtained using the F673N filter (Kim et al. 2015). The dashed red line denotes the location of the velocity jump in $H\alpha$ (Kim et al. 2017). The positional uncertainties of the WHT and *HST* images are approximately $0''.15$.

5×10^{40} erg s^{-1}) are still regarded as IMBH candidates (e.g. HLX-1; Farrell et al. 2009, HLX-2; Jonker et al. 2010; Heida et al. 2015, M82-X1; Kaaret et al. 2001, and NGC 2276-3c; Sutton et al. 2012; Mezcua et al. 2013).

The interesting ULX (CXO J133815.6+043255) was identified in NGC 5252, a type 2 Seyfert lenticular galaxy. The ULX is $22''$ (≈ 10 kpc) away from the centre of NGC 5252 and has an X-ray luminosity $L_{X\text{-ray}} \approx 1.2 \times 10^{40}$ erg s^{-1} (Kim et al. 2015). Previous studies using spectroscopic data suggest the ULX is kinematically associated with the host with velocity offset of ≈ 13 km s^{-1} (Kim et al. 2015, 2017). Ionized gas appears to be dynamically associated with the ULX, again implying that the ULX is not a background AGN (Kim et al. 2017). Based on the multi-wavelength dataset, the ULX can be explained as an IMBH with a mass of $10^{4-6} M_{\odot}$ (Kim et al. 2015; Mezcua et al. 2018).

However, the nature of the ULX remains unclear. The host galaxy does not show morphological signs of an ongoing merger from optical images, although the complex gas distribution could suggest the host may have undergone a recent minor merger (Prieto & Freudling 1996). Therefore, it is natural to suggest that the ULX is the remnant core of a dwarf galaxy. The dynamical mass of the ULX counterpart as derived from the rotating ionized gas surrounding the ULX, is $\approx 10^{7.5} M_{\odot}$ supporting such a scenario (Kim et al. 2017). However, we cannot rule out that the ULX is a recoiling BH. A key physical parameter to answer this question is the stellar mass associated with the ULX. Therefore, in this paper we present near-infrared (NIR) photometric data for the ULX CXO J133815.6+043255, and we use it to estimate the stellar mass. We then discuss the physical origin of the ULX. We assume the luminosity distance to NGC 5252 is 104 Mpc throughout the paper.

2 OBSERVATIONS AND DATA REDUCTION

To obtain JHK_s imaging of the ULX we used the Long-slit Intermediate Resolution Infrared Spectrograph (LIRIS) mounted on the William Herschel Telescope (WHT). LIRIS has a field of view of $4'.27 \times 4'.27$ and a pixel scale of

$0''.25/\text{pixel}$. The J -band observations were obtained using 11 repetitions of an 8-point-dither pattern where 5 images of 20 s exposure each were taken at each point; the H -band observations used 16 repetitions of the same pattern and the K_s -band observations were performed with 22 repetitions of said pattern. The ULX was observed in the H -band on 2018 March 28, in the J -band on 2018 March 29 and in the K_s -band on 2018 March 30.

Data reduction was performed using the THELI pipeline (Schirmer 2013), which produces a master flat in order to flat-field correct the data. It also generates a sky background model that is then subtracted from each individual image. THELI uses SExtractor Bertin & Arnouts (1996) to detect sources in each frame and finds an astrometric solution using SCAMP (Bertin 2006), the latter is achieved by matching detected source positions to objects from the 2 Micron All Sky Survey (2MASS; Skrutskie et al. 2006). The global astrometric solution is then used for the coaddition of all data frames using SWARP (Bertin et al. 2002). The astrometric uncertainty is estimated to be $\sim 0''.15$, which is comparable to that of *Hubble Space Telescope* (*HST*) images (Kim et al. 2015).

The photometric zero-point was defined by comparing the photometric results from our imaging data with those from UKIRT Infrared Deep Sky Survey (UKIDSS; Lawrence et al. 2012) for the same stars. We performed aperture photometry for our dataset using the same aperture radius ($4''$) as the UKIDSS data. Because the UKIDSS data is shallower than ours, we only used stars brighter than 18.5 mag for J and H bands and 17.5 mag for the K_s -band for the comparison. Excluding objects with nearby companions, 10–20 stars were finally used. The uncertainties in the zero-point were 0.03, 0.06, and 0.06 mags in J , H , and K_s , respectively. Throughout this paper, all the magnitudes are in the Vega system.

3 PHOTOMETRIC PROPERTIES

3.1 Photometry

The ULX was clearly detected in all the three bands (Fig. 1). Because the ULX resides in the host galaxy outskirts, it is

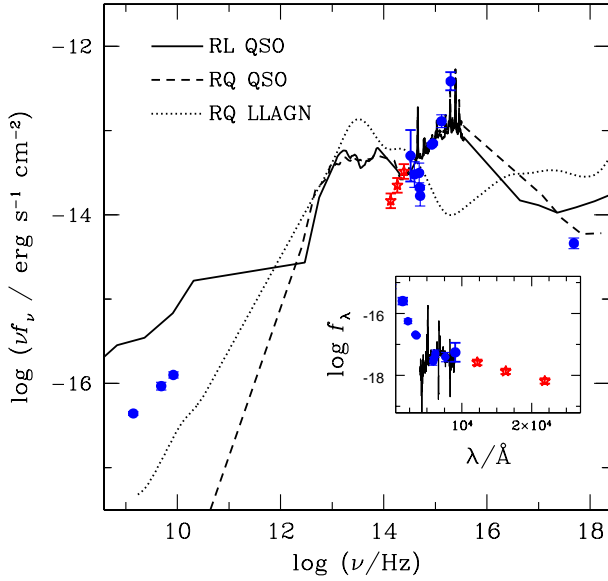


Figure 2. The spectral energy distribution for CXO J133815.6+043255. Blue points are from Kim et al. 2015 and references therein; red points are photometric measurements from our NIR images; solid, dashed, and dotted lines denote the template SEDs for radio-loud QSOs, radio-quiet QSOs, and radio-quiet low-luminosity AGNs, respectively. Inset: Optical-NIR SED; the solid line represents the optical spectrum of the ULX (Kim et al. 2015); the units on the Y-axis (f_λ) are $\text{erg cm}^{-2} \text{s}^{-1} \text{\AA}^{-1}$.

not straightforward to measure the ULX brightness. Therefore, we performed photometry using three different methods. Aperture photometry with an aperture radius of 2 and 4 arcsec provided magnitudes for the NIR counterpart of the ULX. These are 20.36–20.77, 19.68–20.01, and 19.45–19.77 at J , H , and K_s , respectively. Besides, AUTO magnitudes were measured by SExtractor, with $J = 20.19$, $H = 19.81$, and $K = 19.44$. Finally, we used GALFIT (Peng et al. 2002) to properly remove the background gradient caused by the host galaxy, modelling the NIR counterpart with a point spread function (PSF). We used ~ 50 – 100 stars to construct the PSF for each image, yielding $J = 20.93$, $H = 19.97$, and $K = 19.52$. Overall, the brightness from the various methods shows a rough agreement within an uncertainty of 0.2–0.3 mag. These uncertainties were considered when we below calculated the error in the stellar mass. We adopt the AUTO magnitude in the following discussion.

We used GALFIT to model the target with an Sérsic function (Sérsic 1968) to estimate the the NIR counterpart physical size of the ULX. However, we found that the source was unresolved in all three images. The full-width at half maximum for the target ($\sim 0''.7$) was comparable with that for the field stars, implying that the target is physically smaller than ≈ 0.3 kpc, which is consistent with the finding from the optical counterpart (Kim et al. 2015).

3.2 The stellar mass and population

The UV/optical continuum can be dominated by light from accretion onto the BH. Thus, the NIR photometry is crucial to estimate the stellar mass associated with the ULX. We used the $H - K_s$ colour to infer the mass-to-light ratio in the K_s -band magnitude because those filters are less affected by emission from the accretion disk. We adopted the conversion factor from Bell & de Jong (2001), yielding $\log M_{*,\text{ULX}} = 7.90 \pm 0.10 M_\odot$. The stellar mass derived using $J - K_s$ ($\log M_{*,\text{ULX}} = 7.25 \pm 0.10 M_\odot$) is smaller than that from $H - K_s$. This may indicate that J -band is somewhat affected by the continuum from the accretion, making the ULX bluer (implying a smaller mass-to-light ratio). The IR continuum from a dusty torus can partly contribute to the K_s -band flux. But we found no clear sign of an IR bump from the spectral energy distribution (SED) of the ULX (Fig. 2), suggesting that the light from the torus may be small or even negligible. This is discussed further in SS4.2. Nevertheless, the stellar mass derived from our NIR photometry can be regarded as an upper limit considering a potential contribution from an accretion disk and dusty torus.

Adopting a simple stellar population model from Bruzual & Charlot (2003), the observed NIR colour ($H - K_s \sim 0.37$) can be reproduced by old and intermediate-age stars ($\sim 10^8$ – 10^{10} yr) with supersolar metallicity ($[\text{Fe}/\text{H}] \geq 0$). This suggests that the stellar component of the progenitor associated with the ULX may arise from a massive system, as inferred from the mass-metallicity relation (Tremonti et al. 2004). On the other hand, the $J - H$ and $J - K_s$ colours suggest the NIR light could be generated by intermediate-age stars ($\sim 10^8$ – 10^9 yr), regardless of their metallicity, which would not require the progenitor to be overly massive. It is difficult to draw solid conclusions without knowing the exact contribution to the brightness from the accretion disk and torus.

4 OFF-NUCLEAR BLACK HOLE ORIGIN

4.1 Merging dwarf galaxy?

Previous studies regarded the ULX in NGC 5252 as an IMBH candidate for several reasons. Optical images of NGC 5252 show no evidence for recent interaction, suggesting the ULX was less likely to be the nucleus of a massive merging galaxy (i.e. SMBH; Kim et al. 2015). The dynamical mass derived from gas kinematics in the vicinity of the ULX is $\approx 4 \times 10^7 M_\odot$ (Kim et al. 2017). In addition, VLBA observations of the ULX showed the BH mass was as large as $10^6 M_\odot$ (Mezcua et al. 2018). For that calculation, the BH mass was inferred from the correlation between the X-ray luminosity, BH mass, and radio luminosity (the BH fundamental plane of activity, Merloni et al. 2003). Although the radio luminosity is measured from the radio core, this BH mass can be regarded as an upper limit because the contribution from the star formation is unknown.

The derived stellar mass ($\log M_* = 7.90 M_\odot$) provides additional clues for the origin of the ULX. Considering the upper limit on the physical size of the stellar component estimated from NIR data (≤ 0.3 kpc), the stellar properties (size and stellar mass) in the vicinity of the ULX are comparable to those for ultra-compact dwarfs (UCDs;

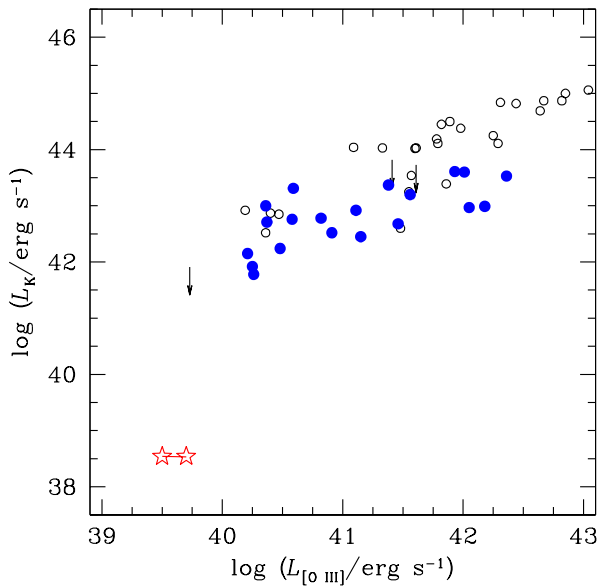


Figure 3. Nuclear K_s -band luminosity plotted against the [O III] luminosity for AGNs. Open and filled circles denote type 1 and 2 AGNs, respectively (Alonso-Herrero et al. 1997). The K_s -band luminosity for most targets was measured from the nucleus with 3 – 6 arcsec aperture radii. AGNs with upper limit on the K_s -band luminosity are shown with arrows. The red stars represent the ULX in NGC 5252. Because the [O III] luminosity of the ULX can be overestimated due to the extended features, we set a lower limit on it using aperture photometry with $0''.5$ radius for IFU data obtained with GMOS (Kim et al. 2017).

Fahrion et al. 2019) rather than conventional bulges. Nevertheless, if we assume the ULX is associated with stellar bulges, the BH mass is $\approx 10^5 M_\odot$, using the correlation between black hole mass and stellar mass (Kormendy & Ho 2013). However, there are three caveats for this calculation. First, the BH-host mass relation was derived from the normal galaxies with $M_* > 10^9 M_\odot$, and it is unknown if the correlation holds for less massive galaxies (e.g. Davis et al. 2018, 2019; Schutte et al. 2019; Woo et al. 2019). Second, the correlation appears to be tight only for elliptical galaxies and classical bulges. For pseudo-bulges, the BH tends to be undermassive compared to classical bulges for a given bulge mass (e.g. Ho & Kim 2014). If the ULX was hosted by a pseudo bulge, the expected BH mass can be even smaller than $10^5 M_\odot$. Finally and most importantly, the stellar component accompanied by the ULX could have been tidally stripped by the interaction with NGC 5252, as suggested from observational studies of UCDs (e.g. Seth et al. 2014; Ahn et al. 2017; Afanasiev et al. 2018). This is also consistent with the apparent supersolar metallicity for stars in the vicinity of the ULX estimated from the $H-K_s$ colour. UCDs lies above the mass-metallicity relation, suggesting that part of the stellar mass of their progenitors was stripped off (e.g. Zhang et al. 2018). The stellar metallicity for massive UCDs (e.g., M60-UCD1 and M59-UCD3) is comparable to that for the NIR counterpart of the ULX.

In massive UCDs, the central SMBH mass can be as high as $\sim 20\%$ of the host stellar mass. Adopting this limit,

the BH mass can be up to $\approx 10^{6-7} M_\odot$, which is in good agreement with the mass derived using the BH fundamental plane of activity. If the ULX is the remnant of a merging dwarf galaxy, and the BH mass $\approx 10^6 M_\odot$ as suggested by the BH fundamental plane of activity, the host galaxy progenitor of the ULX is expected to be as massive as $\approx 5 \times 10^8 M_\odot$. Thus, more than 30% of the stellar mass has been stripped off, probably during the merger.

Kim et al. (2017) concluded that the dynamical mass for this system is $\approx 4 \times 10^7 M_\odot$ using the ionized gas rotation in the vicinity of the ULX. Although this measurement is somewhat uncertain due to the unknown inclination angle, it can be regarded as an approximate upper limit for the BH mass. Intriguingly, the measured stellar mass is consistent with the dynamical mass. Hence, the BH mass could be significantly smaller than the dynamical mass, implying that the ULX can be associated with an IMBH. However, the location of the velocity jump is offset from the positions of the ULX and NIR counterpart (red dashed line in Fig 1). This may indicate that the velocity jump is not due to the rotation but instead represents the edge of two ionized gas clouds with distinct velocities. Therefore, the dynamical mass calculated assuming the sharp transition in the velocity is due to the rotation may not reflect the actual mass of the system associated with the ULX.

4.2 The lack of dusty torus

The NIR light in AGNs can be emitted not only by stars in the host galaxy, but also by a hot dusty torus, and the NIR band contribution from the accretion disk may be non-negligible for type 1 AGNs (e.g. Hernán-Caballero et al. 2016). Thus, the K_s -band has been widely used to explore the physical properties of torus (e.g. Alonso-Herrero et al. 1996; Koshida et al. 2014). Fig. 3 shows a weak correlation between the [O III] luminosity and the nuclear K_s -band luminosity for various AGN types. The nuclear K_s -band luminosity was measured using aperture photometry, hence the light from the stellar components in bulges may be non-negligible. Although the scatter is significant, the reprocessed light from the dust is closely related to the heating source (i.e. AGN luminosity; Alonso-Herrero et al. 1997). The ULX lies substantially below the relation of ordinary AGNs¹. This discrepancy is also present in the comparison of the SED between the ULX and AGNs (Fig. 2), which can be partly explained since the contribution from stars around the ULX is significantly lower than in the case of Seyferts because the ULX stellar component was heavily stripped during the merger. However, this cannot be the whole story as the fraction of light from hot dust in the K_s -band is known to exceed 20% in type 2 Seyferts.

The deficit of K_s -band flux may indicate that a dusty torus is not present around the ULX. A UV excess is prominent in the SED and no significant absorption was detected in the X-ray spectrum: the ULX is similar in that respect to type 1 AGN. In contrast, broad emission lines are *not*

¹ Considering the uncertainty due to the contribution from the extended narrow line region, we show the [O III] luminosity range in Fig. 3.

detected (Kim et al. 2015). The simultaneous absence of evidence for a torus and a broad emission line region (BLR) appears to violate the conventional AGN unification model (e.g. Antonucci 1993), suggesting the ULX could be a “true” type 2 AGN, which intrinsically lack a BLR and torus. Such type 2 AGNs have either a low Eddington ratio with relatively large BH mass (e.g. Tran et al. 2011) or high Eddington ratio (≥ 0.3) with a low-mass non-stellar BH (e.g. Ho et al. 2012; Miniutti et al. 2013). This can be partly explained by a scenario, where the BLR and torus were formed from the wind from the accretion disk (e.g. Elitzur & Ho 2009; Elitzur et al. 2014). Based on multiwavelength studies, the ULX may host a low mass BH in its centre, hence it is likely to have a high Eddington rate (but see Yang et al. 2017).

ACKNOWLEDGEMENTS

We are grateful to the referee, Roberto Soria, for very constructive comments. This research was based on observations made with the William Herschel Telescope operated on the island of La Palma by the Isaac Newton Group in the Spanish Observatorio del Roque de los Muchachos of the Instituto de Astrofísica de Canarias. LCH was supported by the National Science Foundation of China (11721303, 11991052) and the National Key R&D Program of China (2016YFA0400702). This work was supported by the National Research Foundation of Korea (NRF) grant funded by the Korea government (MSIT) (No. 2017R1C1B2002879). PGJ and KML acknowledge funding from the European Research Council under ERC Consolidator Grant agreement no 647208. KML would like to thank Mischa Schirmer for his invaluable help with the data reduction pipeline THELI. MI acknowledges the support from the NRFK grant, No. 2017R1A3A3001362.

REFERENCES

- Afanasiev A. V., et al., 2018, *MNRAS*, **477**, 4856
Ahn C. P., et al., 2017, *ApJ*, **839**, 72
Alonso-Herrero A., Ward M. J., Kotilainen J. K., 1996, *MNRAS*, **278**, 902
Alonso-Herrero A., Ward M. J., Kotilainen J. K., 1997, *MNRAS*, **288**, 977
Antonucci R., 1993, *ARA&A*, **31**, 473
Bañados E., et al., 2018, *Nature*, **553**, 473
Bachetti M., et al., 2014, *Nature*, **514**, 202
Bell E. F., de Jong R. S., 2001, *ApJ*, **550**, 212
Bertin E., 2006, in Gabriel C., Arviset C., Ponz D., Enrique S., eds, *Astronomical Society of the Pacific Conference Series Vol. 351, Astronomical Data Analysis Software and Systems XV*. p. 112
Bertin E., Arnouts S., 1996, *A&AS*, **117**, 393
Bertin E., Mellier Y., Radovich M., Missonnier G., Didelon P., Morin B., 2002, in Bohlender D. A., Durand D., Handley T. H., eds, *Astronomical Society of the Pacific Conference Series Vol. 281, Astronomical Data Analysis Software and Systems XI*. p. 228
Brightman M., et al., 2018, *Nature Astronomy*, **2**, 312
Bruzual G., Charlot S., 2003, *MNRAS*, **344**, 1000
Davis B. L., Graham A. W., Cameron E., 2018, *ApJ*, **869**, 113
Davis B. L., Graham A. W., Cameron E., 2019, *ApJ*, **873**, 85
Elitzur M., Ho L. C., 2009, *ApJ*, **701**, L91
Elitzur M., Ho L. C., Trump J. R., 2014, *MNRAS*, **438**, 3340
Fahrion K., et al., 2019, *A&A*, **625**, A50
Farrell S. A., Webb N. A., Barret D., Godet O., Rodrigues J. M., 2009, *Nature*, **460**, 73
Fürst F., et al., 2016, *ApJ*, **831**, L14
Greene J. E., Ho L. C., 2004, *ApJ*, **610**, 722
Heida M., et al., 2015, *MNRAS*, **453**, 3510
Hernán-Caballero A., Hatziminaoglou E., Alonso-Herrero A., Mateos S., 2016, *MNRAS*, **463**, 2064
Ho L. C., Kim M., 2014, *ApJ*, **789**, 17
Ho L. C., Kim M., Terashima Y., 2012, *ApJ*, **759**, L16
Israel G. L., et al., 2017, *Science*, **355**, 817
Jonker P. G., Torres M. A. P., Fabian A. C., Heida M., Miniutti G., Pooley D., 2010, *MNRAS*, **407**, 645
Kaaret P., Prestwich A. H., Zezas A., Murray S. S., Kim D.-W., Kilgard R. E., Schlegel E. M., Ward M. J., 2001, *MNRAS*, **321**, L29
Kim M., et al., 2015, *ApJ*, **814**, 8
Kim M., Ho L. C., Im M., 2017, *ApJ*, **844**, L21
King A. R., Davies M. B., Ward M. J., Fabbiano G., Elvis M., 2001, *ApJ*, **552**, L109
Kormendy J., Ho L. C., 2013, *ARA&A*, **51**, 511
Koshida S., et al., 2014, *ApJ*, **788**, 159
Lawrence A., et al., 2012, *VizieR Online Data Catalog*, p. II/314
Merloni A., Heinz S., Di Matteo T., 2003, *MNRAS*, **345**, 1057
Mezcua M., 2017, *International Journal of Modern Physics D*, **26**, 1730021
Mezcua M., Roberts T. P., Sutton A. D., Lobanov A. P., 2013, *MNRAS*, **436**, 3128
Mezcua M., Kim M., Ho L. C., Lonsdale C. J., 2018, *MNRAS*, **480**, L74
Miller B. P., Gallo E., Greene J. E., Kelly B. C., Treu T., Woo J.-H., Baldassare V., 2015, *ApJ*, **799**, 98
Miniutti G., Saxton R. D., Rodríguez-Pascual P. M., Read A. M., Esquej P., Colless M., Dobbie P., Spolaor M., 2013, *MNRAS*, **433**, 1764
Mortlock D. J., et al., 2011, *Nature*, **474**, 616
Peng C. Y., Ho L. C., Impey C. D., Rix H.-W., 2002, *AJ*, **124**, 266
Prieto M. A., Freudling W., 1996, *MNRAS*, **279**, 63
Schirmer M., 2013, *ApJS*, **209**, 21
Schutte Z., Reines A., Greene J., 2019, arXiv e-prints, p. arXiv:1908.00020
Sérsic J. L., 1968, *Atlas de galaxias australes (Córdoba: Obs. Astron., Univ. Nac. Córdoba)*
Seth A. C., et al., 2014, *Nature*, **513**, 398
She R., Ho L. C., Feng H., 2017, *ApJ*, **842**, 131
Skrutskie M. F., et al., 2006, *AJ*, **131**, 1163
Sutton A. D., Roberts T. P., Walton D. J., Gladstone J. C., Scott A. E., 2012, *MNRAS*, **423**, 1154
Swartz D. A., Ghosh K. K., Tennant A. F., Wu K., 2004, *ApJS*, **154**, 519
Tran H. D., Lyke J. E., Mader J. A., 2011, *ApJ*, **726**, L21
Tremonti C. A., et al., 2004, *ApJ*, **613**, 898
Volonteri M., 2010, *A&ARv*, **18**, 279
Walton D. J., Roberts T. P., Mateos S., Heard V., 2011, *MNRAS*, **416**, 1844
Woo J.-H., Cho H., Gallo E., Hodges-Kluck E., Le H. A. N., Shin J., Son D., Horst J. C., 2019, *Nature Astronomy*, p. 336
Yang X., et al., 2017, *MNRAS*, **464**, L70
Zhang H.-X., et al., 2018, *ApJ*, **858**, 37

This paper has been typeset from a $\text{\TeX}/\text{\LaTeX}$ file prepared by the author.